



Alignment studies for the Belle II tracking system

Jakub Kandra, Charles University in Prague, Czech Republic

September 9, 2015

Abstract

Alignment validation of the Belle II tracking system is discussed. Two validation methods are described: the first based on the use of cosmic-ray tracks and the second based on the reconstruction of a physics process with a high counting rate. The validation procedures are tested with different available event generators and track finding methods.

Contents

1	Introduction	4
2	The Belle II tracking system	4
2.1	Pixel detector	4
2.2	Silicon vertex detector	4
2.3	Central drift chambers	5
3	Alignment validation with $D^{*+} \rightarrow \pi_{slow}^+ D^0(\rightarrow K3\pi)$	6
3.1	Alignment validation procedure	6
4	Alignment validation using cosmic-ray tracks	11
4.1	The CRY generator of cosmic showers	11
4.1.1	Generation algorithm of CRY	11
4.2	Validation procedure	12
4.3	Comparison of track finders	13
4.4	Reference plots for alignment validation	14
5	Conclusion	16

Acknowledgments

I would like to thank my supervisor Sergey Yashchenko for the opportunity to work in the Belle II group at DESY and for his patience during discussions about alignment and tracking system of Belle II and other topics. I would also like to thank Simon Wehle for his introduction to the Belle II framework, alignment validation and providing me with his scripts for faster orientation in the framework. I would like to thanks Torben Ferber for his help in my first steps with the CRY generator and explanations of all settings of the generator. Then I would like to thank Oliver Frost for the introduction to his track finder and CDC. Finally, I would like to thank all members of the Belle II group at DESY for perfect atmosphere during weekly meetings and many helpful questions during discussions.

1 Introduction

Belle II is an experiment under construction in Tsukuba, Japan. Belle II will continue and extend the physics program of Belle, which finished operations in 2010. The main goal of Belle was the study of CP violation in B-meson decays. The Belle II program is extended in several directions, e.g., to the search of new physics in rare processes. Therefore, tracking measurements with very high precision are important. It is achieved at Belle II using silicon pixel and strip vertex detectors and a central drift chamber. Precise knowledge about positions and orientations of these detector is very important. For this purpose, a common alignment and calibration procedure using Millepede II [1] is currently under development. After alignment and calibration parameters of the detectors are determined it is necessary to check if the achieved accuracy is enough for the physics analysis. An alignment validation procedure under development [2] is based on the analysis of cosmic-ray tracks and a decay with a high counting rate. Several studies leading to the further development and improvement of the validation procedure are performed in the Belle II analysis framework basf2 and described in the report.

2 The Belle II tracking system

Belle II studies B physics at high luminosity [3]. For production of B mesons, asymmetric electron-positron collisions are utilized at SuperKEKB. Electrons with the energy of 7 GeV are collided with 4 GeV positrons. The tracking system of Belle II (see Fig. 1) consists of a pixel (PXD) and a silicon-strip detector (SSD) and a central drift chamber (CDC).

2.1 Pixel detector

For detection of the produced particles near the interaction point, a pixel detector (PXD) will be used. It is located 14 mm from the interaction point. Because of extreme luminosity, necessity of very precise vertex reconstruction and requirement of minimalistic material budget, the PXD is made using DEPFET (DEPleted Field Effect Transistor) technology [4]. It is a semiconductor detector concept that combines detection and amplification in one device. The technology allows the production of very thin (50 μm) sensors. The DEPFET technology is used for photon science, X-ray images and particle trackers [5]. The PXD consists of two layers: the first layer containing 8 sensors with a size of $15 \times 100 \text{ mm}^2$ and pixel size of $50 \times 50 \mu\text{m}^2$ and the second layer having 12 sensors with the size of about $15 \times 120 \text{ mm}^2$ and pixels of $50 \times 75 \mu\text{m}^2$.

2.2 Silicon vertex detector

Next to the PXD detector, a silicon strip detector (SVD) is located. The SVD should be mechanically stable, has low mass and operates reliably and with very low dead time in the presence of beam background. It consists of 4 layers and 49 ladders at radii of

38, 80, 115 and 140 mm . Two different types of sensor shape are used: a rectangular sensors, which will be installed at the barrel part, and a trapezoidal-shape sensors to cover the forward region. The layers are composed by 16, 30, 56 or 85 sensors in each layer.

2.3 Central drift chambers

The outermost tracking detector is a central drift chamber (CDC). It plays three important roles: the reconstruction of tracks, the measurement of their momenta and the particle identification using energy deposits in the gas volume. It is designed as concentric cylinders with the inner radius of 160 mm and the outer radius of 1130 mm . The height of CDC is 2.4 m . In CDC, there are 14 336 sense wires in 56 layers. The diameter of wires is 30 μm and the gas mixture is He-C₂H₆.

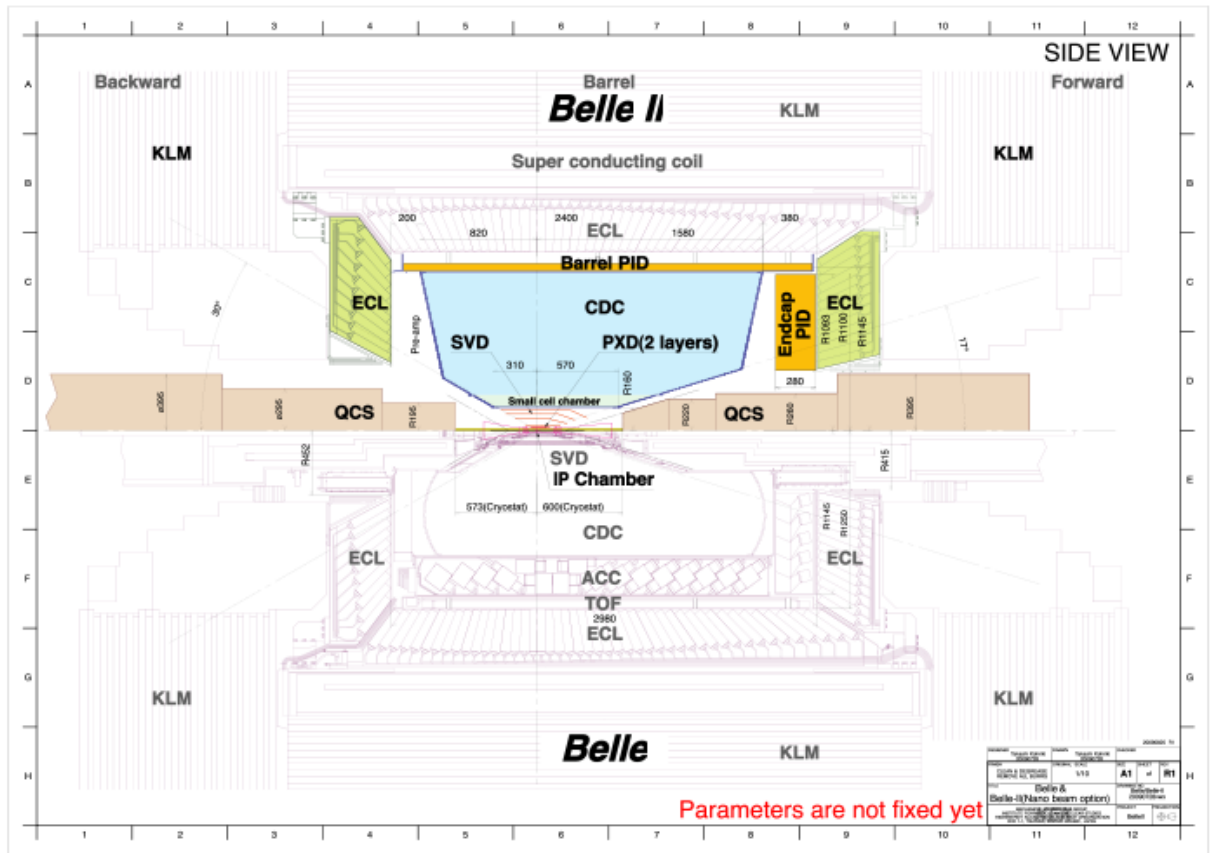


Figure 1: The design of the Belle II detector (top) compared to Belle (bottom).

3 Alignment validation with $D^{*+} \rightarrow \pi_{slow}^+ D^0 (\rightarrow K3\pi)$

For validation of alignment and calibration, one can select events from a well-studied physics process with a high counting rate and physics distributions that can be used as references. One of such processes is a decay of D^{*+} to D^0 and a positively charged pion π_{slow} with very small momentum (see Fig. 2). The neutral D^0 is not stable and decays to four particles: two positively charged π^+ , negatively charged π^- and a K^- . This decay of D^0 is referred to “K3 π ” in the following.

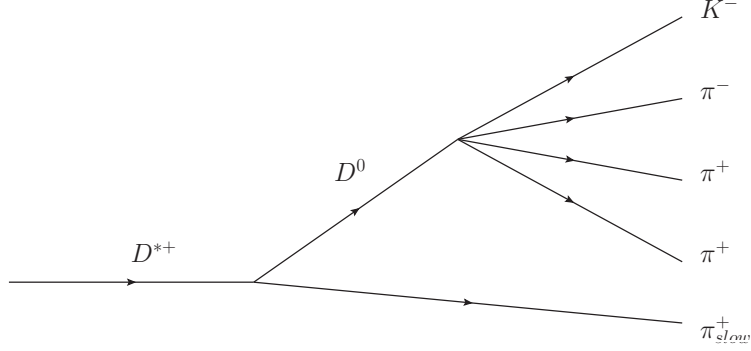


Figure 2: A decay chain $D^{*+} \rightarrow \pi_{slow}^+ D^0 (\rightarrow K3\pi)$.

3.1 Alignment validation procedure

In the analysis, only one produced D^{*+} per event is used. In the detectors we observe five charged particles. From tracking detectors, momenta and positions of particles in the final state are reconstructed (see Fig. 3). For the reconstruction of D^0 , we use pairs of particles and reconstruct their vertices from particles with the same charge $((+ \times +) \times (- \times -))$ and particles with different charges $((+ \times -) \times (+ \times -))$. In Fig. 4 residuals defined as differences between each component of the vertex positions are presented. These residuals will be used as reference polts. From kinematic parameters of the reconstructed particles one can calculate invariant mass of D^0 (Fig. 5) and the the sum of momenta of produced particles (Fig. 6). The invariant mass is fitted using three different functions (Gaussian, Breit-Wigner, and Crystal ball as a signal and Chebyshev function of the second order as a background). The result of fitting with the smallest χ^2 are used in the analysis and shown in the figures. From the kinematic parameters of all reconstructed particles, including the pion with low momentum (Fig. 6), the invariant mass of D^{*+} is reconstructed (Fig. 7). In the validation procedure, two conditions for better selection of the signal decay and rejection of the background are used (Fig. 8).

1. Sum of momenta of produced particles from D^0 decay is required to be in the interval between 2.5 and 6.0 GeV.

2. Invariant mass of D^{*+} is required to be in the range of two standard deviations from the mean value of the fitted function.

The results of the analysis are shown in Fig. 9. This plot will be used as a reference plot for alignment validation.

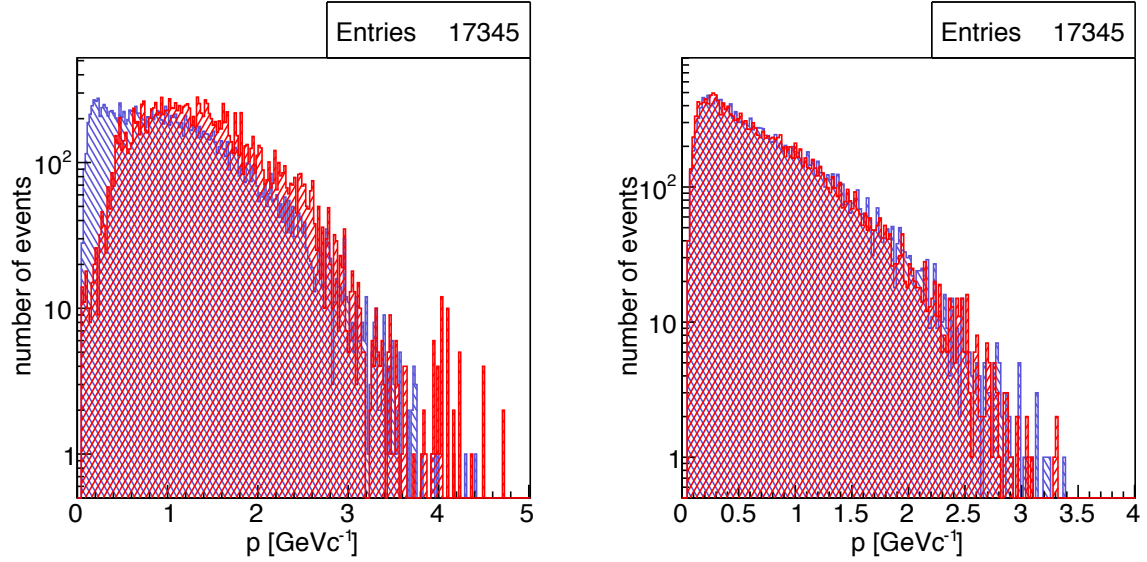


Figure 3: Momenta of produced particles from $K3\pi$ decay for positively charged pions (blue), negatively kaon (left panel, red) and negatively charged pion (right panel, red).

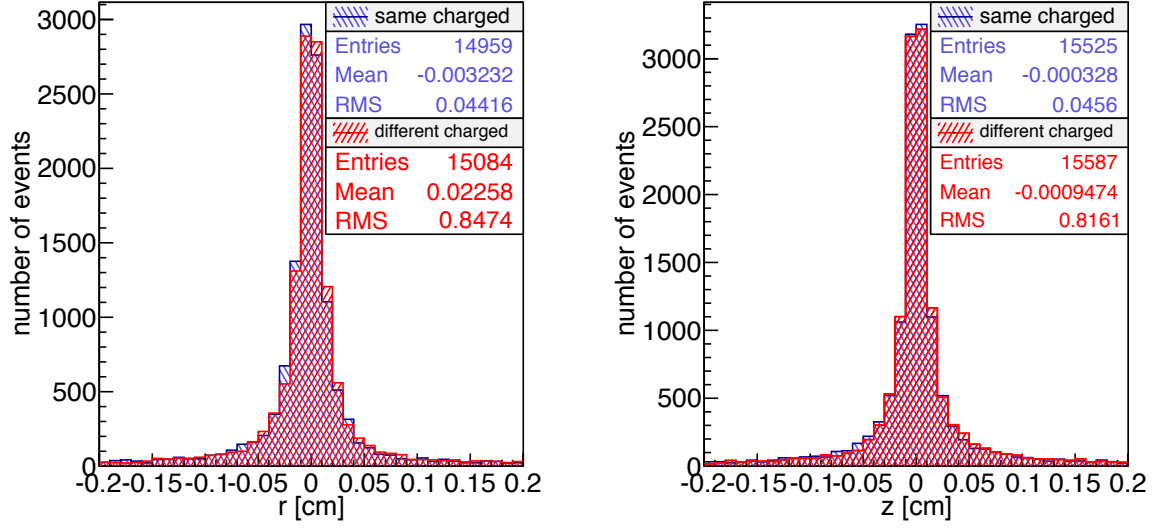


Figure 4: Residuals of reconstructed vertices in r-component of cylindrical system (left panel) and in z-component (right panel) for particles with the same charge (blue) and the particles with different charges (red).

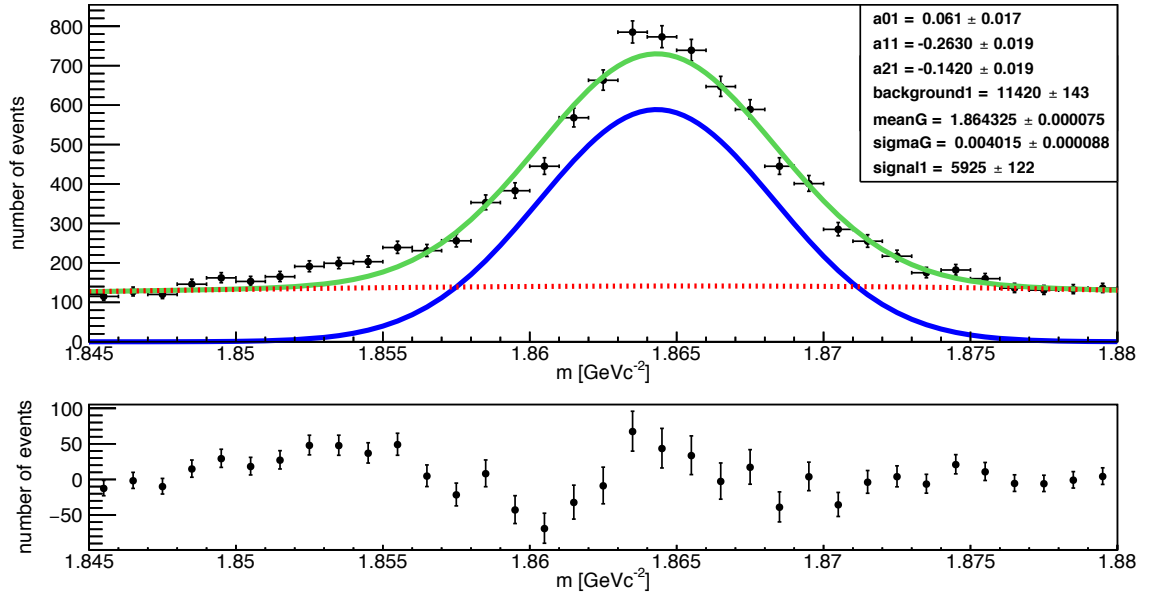


Figure 5: Invariant mass of D^0 (top panel): fitted data (black points), a signal (Gaussian blue curve), a background (dotted red curve) and the sum of the signal and the background (green). Residual of the fit (bottom panel).

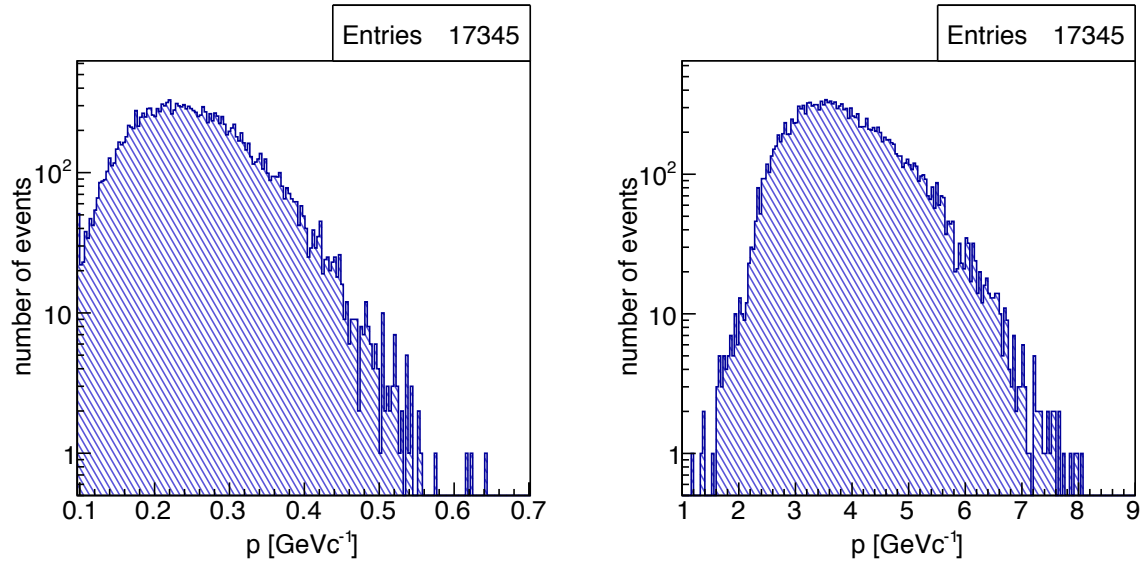


Figure 6: Momentum of π_{slow}^+ (left panel) and the sum of momenta of produced particles from D⁰ decay (right panel).

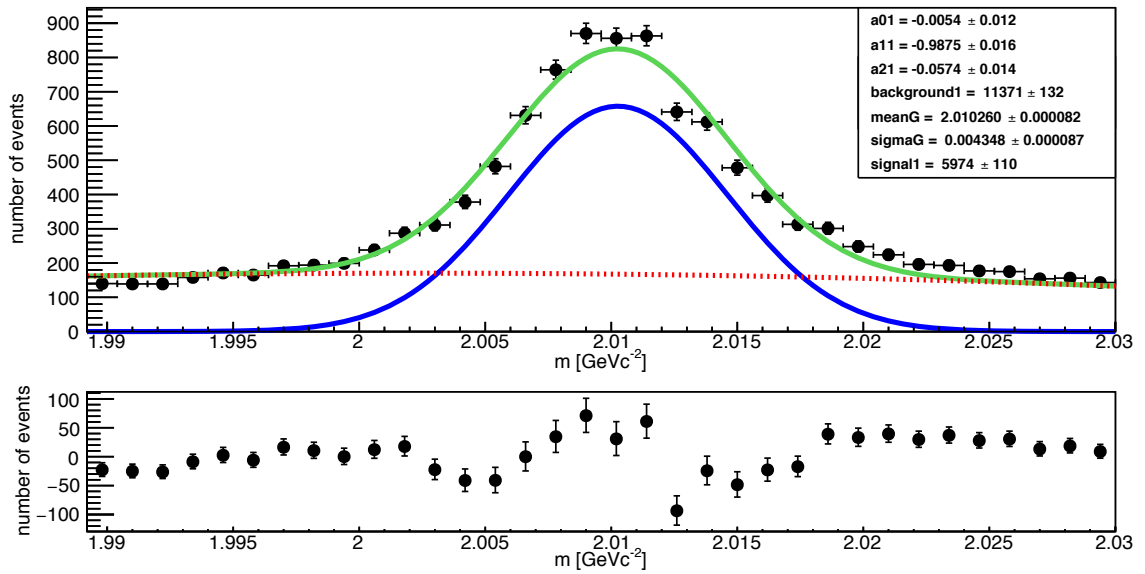


Figure 7: Invariant mass of D^{*+} (top panel): data (black points), a fitted **signal** (Gaussian blue curve), a **background** (dotted red curve) and the **sum of the signal and the background** (green). Residuals of the fit (bottom panel).

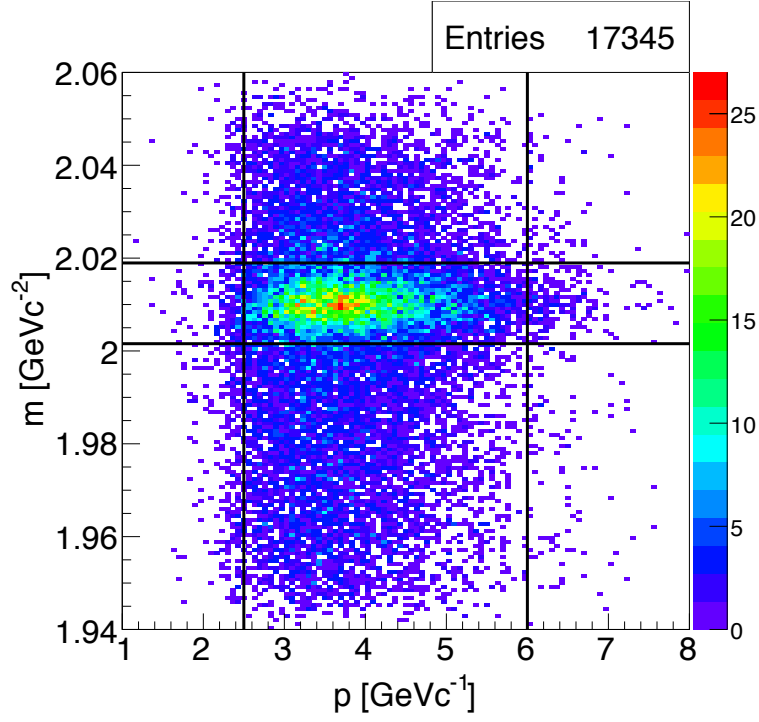


Figure 8: Conditions for signal selection: mass of D^{*+} as a function of the sum of momenta of produced particles from D^0 decay.

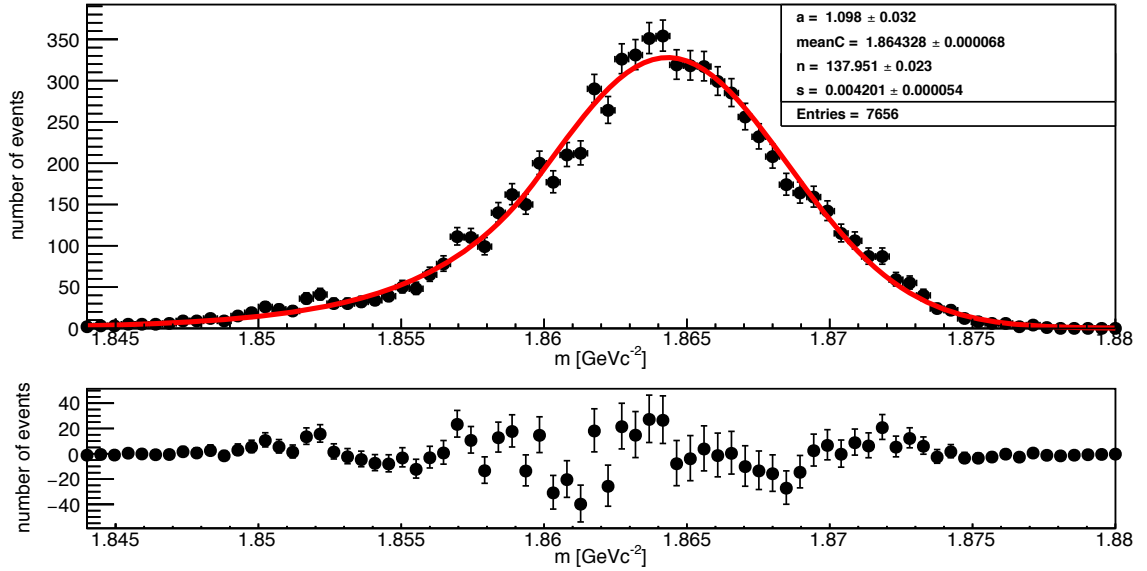


Figure 9: Invariant mass of D^0 after the selection (top panel): fitted data (black points) and the **signal** (Crystal ball red curve). Residuals of the fit (bottom panel).

4 Alignment validation using cosmic-ray tracks

One can use cosmic particles (mainly muons) for alignment and calibration of tracking detectors, because muons pass through all the tracking detectors at different angles and can be detected in the Belle II tracking system. In the magnetic field, cosmic muon trajectories can be approximated by helices, therefore, track finding methods can be easily tested.

4.1 The CRY generator of cosmic showers

For simulation of cosmic rays we use Monte Carlo simulation of proton-induced cosmic-ray cascades in the atmosphere (CRY) [6] used in muon tomography [7], neutrino experiments [8] and development of cosmic shielding materials [9]. It is based on generation of showers from primary protons in the energy range of 1 GeV - 100 TeV. The generated secondary particles are protons, neutrons, pions, muons, electrons and photons. The generator takes period of solar cycle into account and can determine elapsed time in the simulation.

4.1.1 Generation algorithm of CRY

Because a lot of particles are generated in cosmic showers, the simulation of all secondary particles would require a lot of computing time. The authors of CRY developed a system of tables used during the generation. For generation of secondary particles in a specific place on the Earth one needs to define a place of simulation. First step of the algorithm of CRY is a generation of showers from primary particles. After the showers are created, secondary particles are extrapolated into a “generation square” (see Fig. 10). In the next step, the algorithm uses particles from the generation square and reconstructs their trajectories in a “global box”. The following conditions are applied for the reconstructed candidates:

- if any particle is in a “accept box”, the event is accepted,
- all particles that are not in a “keep box” are removed.

The keep box should be larger than or the same as the accept box.

The generation of cosmic rays has the following settings.

1. *Type of secondary particles:* one can choose between types of particles: *neutrons, protons, kaons, pions, muons, electrons* and *photons*.
2. *Altitude of place, which we are interested in:* there are three levels available: the sea level, 2.1 or 11.3 kilometers over the sea level.
3. *Latitude of the place that we are interested in:* the generator permits to set the latitude in the latitude range of $(-90^\circ, 90^\circ)$, where the North Pole is defined as having 90° .

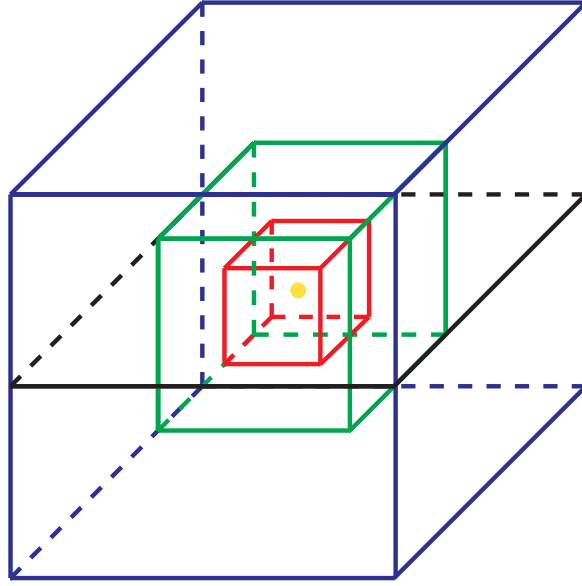


Figure 10: Description of generation boxes: **global box** (blue), **keep box** (green), **accept box** (red), generation plane and **intersection point** (yellow).

4. *Date of the measurement*: this value is connected with the solar cycle.
5. *Kinetic energy threshold for the final particles*.
6. *Sides of the boxes*: as it was explained below, one needs to define three independent boxes.
7. *Side of the generation square*: the setting of plane for the generation of particles.

For validation, we generate particles with specific settings: geographical information of the Belle II experiment, the volume of the keep and accept boxes the same as a cube with the side of 0.1 m . The global box is set as a cube with the side of 50.0 m and the generation plane is defined with the side of 30 m . We perform the simulation using all secondary particles and their minimum kinetic energy set to 10 MeV . The date is set to 6. June 2017 when cosmic tests of the Belle II detectors are planned.

4.2 Validation procedure

A comparison between the number of generated and reconstructed particles is presented in Fig. 11. The momentum distribution of generated and reconstructed muons is also shown in the figure. Mainly muons are detected in the Belle II tracking system because other particles cannot pass through the Belle II outer detectors.

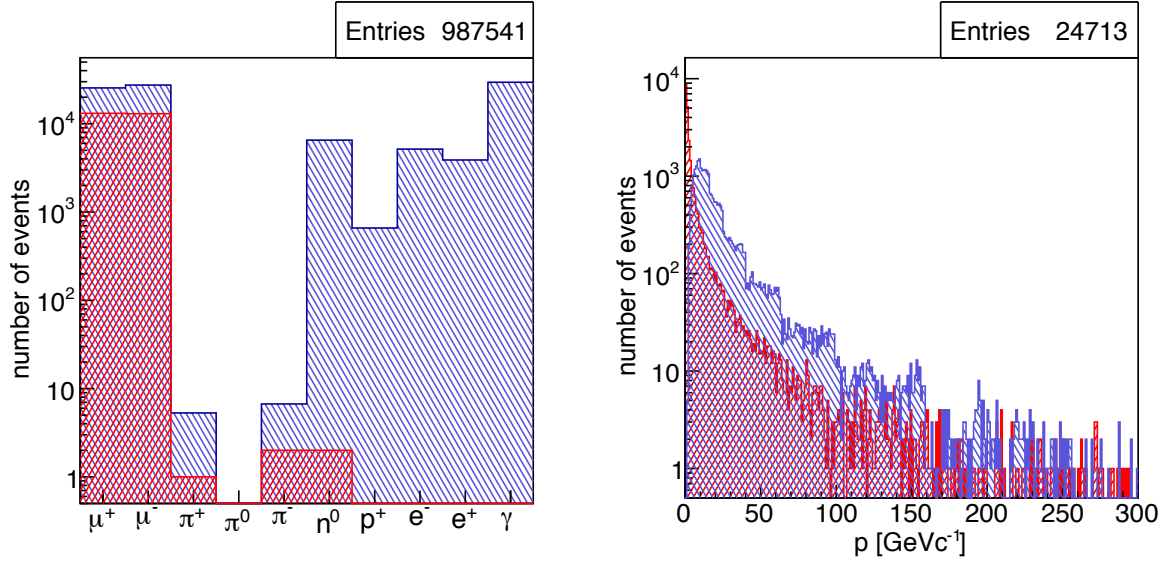


Figure 11: Number of **generated** (blue) and **reconstructed** (red) tracks (left panel) and momentum of **generated** (blue) and **reconstructed** (red) tracks (right panel).

During the cosmic track reconstruction, a track finder Trasan developed for the Belle experiment and implemented in basf2 is used. This track finder was optimized for the search of tracks mainly coming from the interaction region assuming particles propagating from inside the detector to the outside direction. Therefore, for a cosmic track, Trasan finds two tracks: one in the top part of the detector and the other in the bottom part. If a cosmic particle passes the CDC, in most of the cases only one cosmic muon is present and two tracks are found by Trasan. Using the knowledge that these two found tracks are the two parts of the same cosmic muon, one can compare the reconstructed track parameters of two track parts. In case of ideal alignment, the reconstructed track parameters of two track parts should coincide within the track reconstruction uncertainties. Also, because these two track parts are reconstructed independently, there should be no correlations between the track parameters.

4.3 Comparison of track finders

At Belle II, Trasan will be replaced by a more advanced CDC local track finder under development [10] based on a cellular automaton. This track finder is able to find full cosmic tracks without splitting them to two parts. The comparison of two track finders is shown in Tab. 1. The new local track finder is about two times more efficient for cosmic tracks because it does not use any assumption about the origin of the tracks.

	<i>generation</i>	<i>Trasan</i>	<i>CDC local</i>
<i>number of events</i>	1 000 000	10 349	26 146

Table 1: Comparison of two track finders.

4.4 Reference plots for alignment validation

In these studies we define reference plots in order to show the differences between kinematic parameters of these two parts of the track. The reference plot is a matrix, which has the residuals of the track parameters in the diagonal part and the correlations between the track parameters in the non-diagonal part. A color of background in the non diagonal part of the matrix corresponds to the values of correlations (green for $corr \sim 0$ and red for $corr \sim \pm 1$). The residuals are defined as the difference between track parameters of the track parts. The correlations are defined as:

$$corr = \frac{\sum_{i=1}^N (x_i - \bar{x})(y_i - \bar{y})}{\sqrt{\sum_{i=1}^N (x_i - \bar{x})^2} \sqrt{\sum_{i=1}^N (y_i - \bar{y})^2}}. \quad (1)$$

The reference plots for comics validation are shown in Fig. 12 for the Cartesian track parametrization and in Fig. 13 for the helix track parametrization.

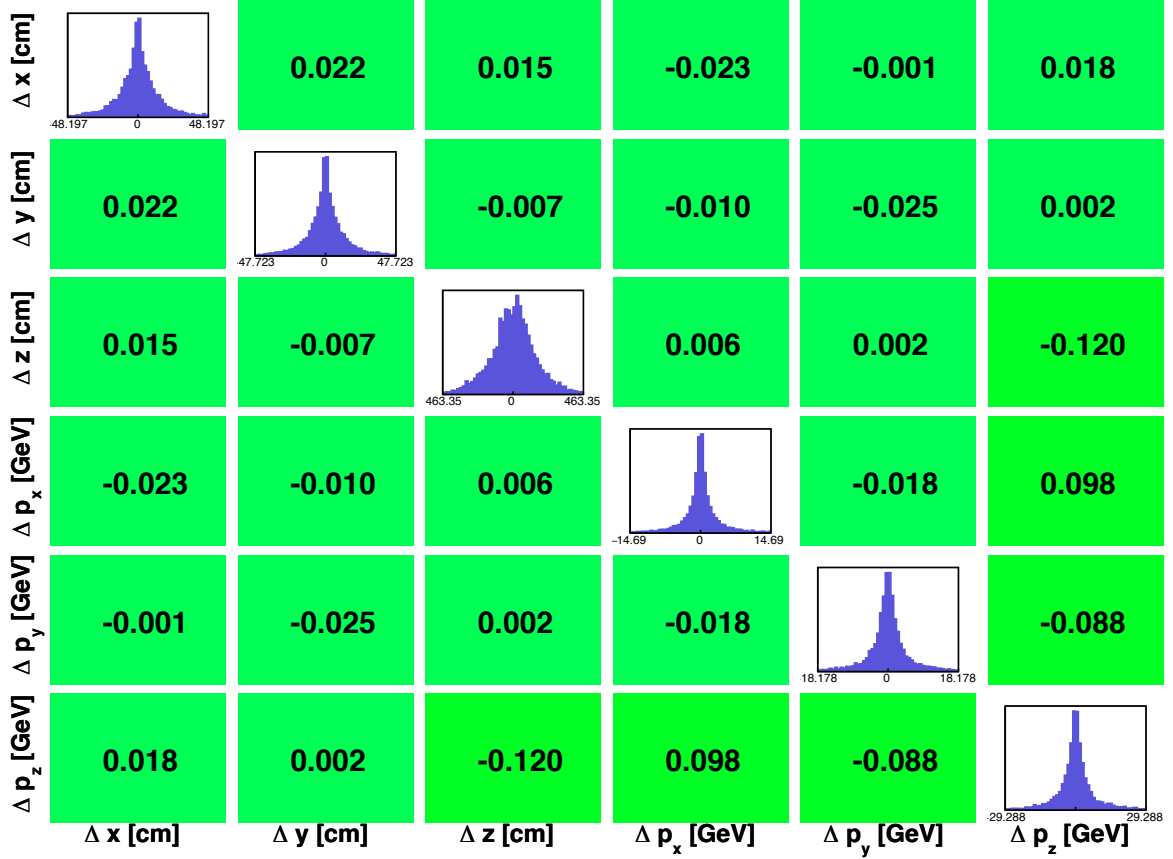


Figure 12: Reference plot for Cartesian coordinates: residuals (diagonal) and correlations (non-diagonal).

In case of misalignment, shifts in the residual distributions can be observed as well as larger correlations between track parameters.

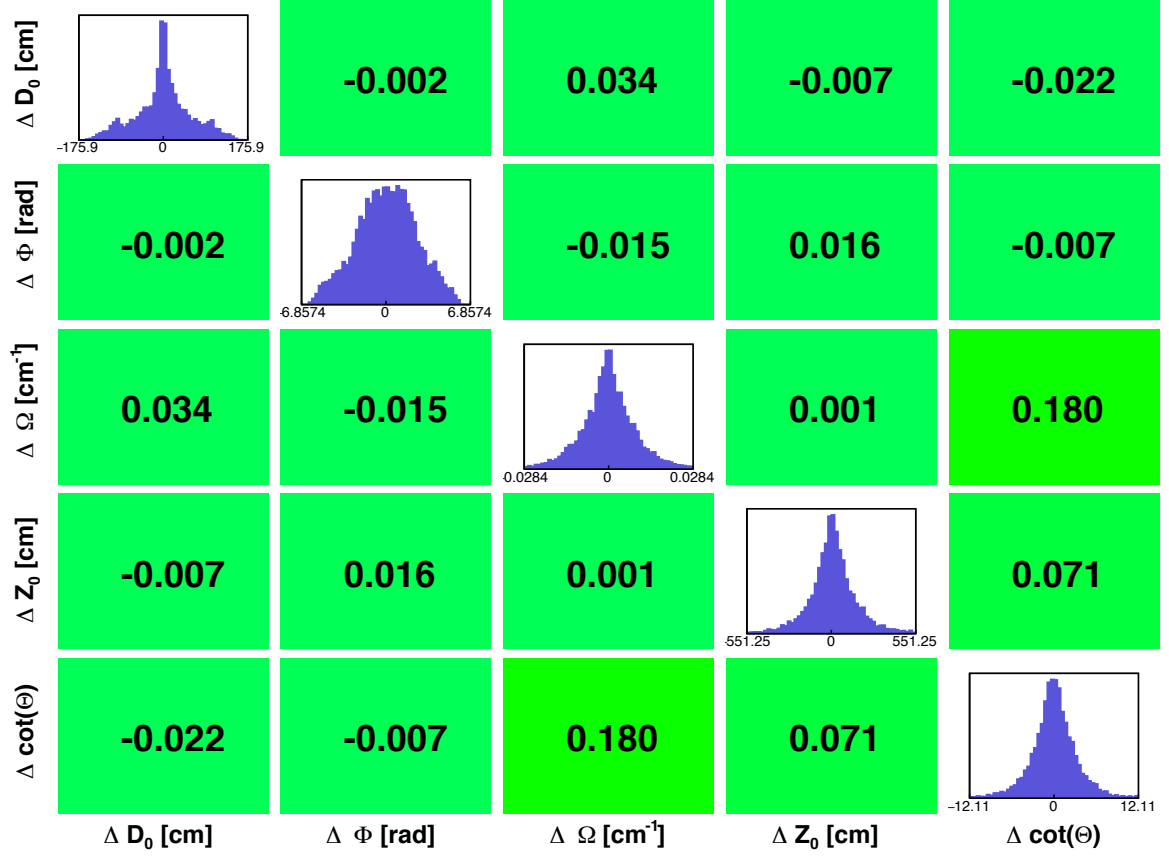


Figure 13: Reference plot for helix parameters: residuals (diagonal) and correlations (non-diagonal).

5 Conclusion

For validation of alignment, two different methods have been studied. First method uses a process with a high counting rate $D^{*+} \rightarrow \pi_{slow}^+ D^0(\rightarrow K3\pi)$. As a result of analysis, three reference plots are defined for this process. Second method uses muons from cosmic rays. With this method, reference validation plots are defined for Cartesian and helix coordinate track representations. The validation procedure have been tested for two different track finding methods. The reference plots will be used in the future study of misalignment and miscalibration effects. In addition, the counting rate from cosmic muons can be estimated for each tracking detector and compared with cosmic calibration measurements using the CRY cosmic-ray generator tested in these studies.

References

- [1] *V. Blobel, C. Kleinwort*: A new method for the high-precision alignment of track detectors, arXiv:hep-ex/0208021
- [2] *S. Wehle*: Private communication
- [3] *Z. Dolezal, S. Uno et al.*: Technical Design Report, arxiv: 1011.0352v1,
- [4] *J. Kemmer and G. Lutz*: Nucl. Instrum. Meth. Phys.Res. A 253, 356 (1987)
- [5] *Max-Planck-Institut fur extraterrestrische Physik and Max-Planck-Institut fur Physik*: Research Activities [online]
- [6] *Ch. Hagmann et al.*: Monte Carlo Simulation of Proton-included Cosmic-ray Cascades in the Atmosphere
- [7] *M. Hohlmann et al.*: GEANT4 Simulation of a Cosmic Ray Muon Tomography System with Micro-Pattern Gas Detectors for Detection of High-Z Materials,
- [8] *E. Niner*: Observation of electron neutrino appearance in the numi beam with the NOVA experiment
- [9] *E. Aguayo et al.*: Cosmic Ray Interaction in Shielding Materials
- [10] *O. Frost*: Private communication